

Long-Term Human Trajectory Prediction using 3D Dynamic Scene Graphs

Nicolas Gorlo, Lukas Schmid, and Luca Carlone

Abstract—We present a novel approach for long-term human trajectory prediction, which is essential for long-horizon robot planning in human-populated environments. State-of-the-art human trajectory prediction methods are limited by their focus on collision avoidance and short-term planning, and their inability to model complex interactions of humans with the environment. In contrast, our approach overcomes these limitations by predicting sequences of human interactions with the environment and using this information to guide trajectory predictions over a horizon of up to 60s. We leverage Large Language Models (LLMs) to predict interactions with the environment by conditioning the LLM prediction on rich contextual information about the scene. This information is given as a 3D Dynamic Scene Graph that encodes the geometry, semantics, and traversability of the environment into a hierarchical representation. We then ground these interaction sequences into multi-modal spatio-temporal distributions over human positions using a probabilistic approach based on continuous-time Markov Chains. To evaluate our approach, we introduce a new semi-synthetic dataset of long-term human trajectories in complex indoor environments, which also includes annotations of human-object interactions. We show in thorough experimental evaluations that our approach achieves a 54% lower average negative log-likelihood (NLL) and a 26.5% lower Best-of-20 displacement error compared to the best non-privileged baselines for a time horizon of 60s.

I. INTRODUCTION

The ability to predict human motion in complex human-centric environments is a crucial component for scene understanding and autonomy, and is prerequisite to a number of applications ranging from consumer, assistive, and care robotics to industrial and retail robots or augmented and virtual reality. Most notably, fulfilling tasks proactively and operating efficiently in human-populated environments, like intercepting a human or moving out of the way proactively, requires reliable predictions of human trajectories over a long time-horizon.

Most current works on human motion and trajectory prediction are primarily motivated by collision avoidance and short-term planning and hence focus on predicting trajectories up to a maximum of 5s [1]–[7]. Thus, trajectories in current benchmark datasets are rarely longer than 10s [8]–[10]. Further, most approaches focus on environments with primarily smooth trajectories, such as outdoor scenes [11]. In contrast, human-centric environments are oftentimes geometrically complex and semantically rich, leading to more complex trajectories.

More rarely and recently, longer prediction horizons up to 30s have been explored [1], [12]. However, even longer

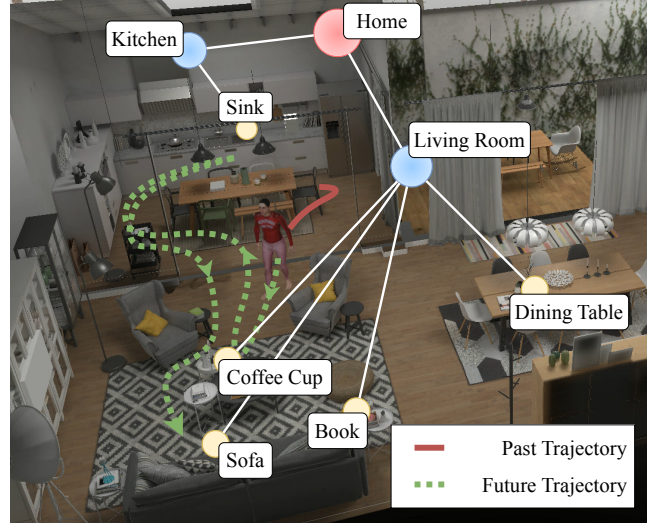


Fig. 1: Our method, LP^2 , predicts a spatio-temporal distribution over long-term (up to 60s) human trajectories in complex environments by reasoning about their interactions with the scene, represented as a 3D Dynamic Scene Graph.

prediction horizons, e.g., up to 60s, are highly beneficial to effective long-term planning and proactive long-term behavior of robots in complex social environments.

Predicting trajectories 60s into the future is a challenging task. First, the aleatoric uncertainty quickly increases with time. Second, the distribution over plausible or even likely human trajectories is highly multi-modal. In addition, humans are much more likely to engage in complex interactions with their environments during longer time horizons which is not well captured by most existing methods. For example, it is feasible to predict human motion if the human follows a corridor, but most methods fail when the human stops to interact with an object in the corridor (e.g., a water dispenser).

To address these challenges, we propose a novel approach to long-term human trajectory prediction called “*Language-driven Probabilistic Long-term Prediction*” (LP^2) that takes such environmental factors into consideration. In contrast to directly predicting human trajectories from past trajectories, we reason about sequences of human interactions with the environment. To this end, we leverage recent developments in 3D dynamic scene graphs (DSGs) [13]–[16] as a scene representation capturing symbolic concepts such as traversability, objects, and agents, as well as advances in Large Language Models (LLMs) for reasoning. LLMs have shown promise in modeling human behavior [17] and anticipating long-term

The authors are with the MIT SPARK Lab, Massachusetts Institute of Technology, Cambridge, USA. {ngorlo, lschmid, lcarlone}@mit.edu

This work was partially supported by Amazon, Lockheed Martin, and the Swiss National Science Foundation (SNSF) grant No. 214489.

actions [18], [19]. We thus leverage LLMs in a novel autoregressive scheme to predict likely interactions with the scene, and propose an approach based on continuous-time Markov chains (CTMC) to infer a probability distribution of the human location across space and time. We further create a novel semi-synthetic dataset of long-term human trajectories in complex indoor environments with rich scene and interaction annotations. We show in thorough experimental evaluations that our approach achieves a 54% lower average negative log-likelihood (NLL) and a 26.5% lower Best-of-20 displacement error compared to the best non-privileged baselines for a time horizon of 60 s.

In summary, we make the following contributions:

- For the first time, we study long-term human trajectory prediction with a prediction horizon of up to 60 s and including complex human-object interactions.
- We present LP^2 , a novel method combining LLM-based zero-shot interaction sequence prediction and CTMC-based probabilistic trajectory prediction to infer multi-modal spatio-temporal distribution over future human positions.
- We introduce a new semi-synthetic dataset of human trajectories in complex indoor environments with annotated human-object interactions. We release our method and data open-source.¹

II. RELATED WORKS

Long-term Human Trajectory Prediction. The problem of long-term human trajectory prediction has attracted notable research interest, and various techniques, ranging from physics-based to pattern-based and planning-based approaches, have been proposed [1]. However, the term "long-term" is often-times used to describe trajectories or joint-level motion of a length of 5 s or less [2], [7], [20], sometimes up to 12 s [21], [22] or rarely up to 30 s [12]. In contrast, we aim to extend this horizon to up to 60 s of prediction.

Recent advances focus on integrating additional input modes like eye-gaze, human joint-level poses [4], or scene context [3], [4], [7], [12]. A group of recent works addresses the problem of social human trajectory forecasting, achieving improved results by modeling the influences of other humans on human trajectories [5]–[7], [23], [24]. However, they typically still focus on a comparably short prediction horizons of 3-20 s and smooth unidirectional motion. In contrast, we address the problem of long-horizon (up to 60 s) trajectory prediction, where complex human-object interactions may lead to sudden stops or changes in walking direction.

Scene Context in Trajectory Prediction. Integrating contextual information about the environment into human trajectory prediction has increased in popularity [2], [4], [5], [7], [12]. Most methods aim to integrate social and environmental clues into the trajectory prediction by feeding geometric scene representations into their pipelines. Common representations include images [5], [7], [12] or occupancy maps [7], [12] of

the global scene, or occupancy maps and LiDAR point clouds of robot observations [4] that are passed to a neural network. These methods predict relatively short trajectories (< 10 s), as the comparably simple environment models may not be detailed enough to reason at a higher level. YNet [12] extends the prediction horizon to up to 30 s by predicting intermediate goals in robot-centered top-down views of the scene [11]. However, the architecture is constrained to a fixed time horizon and predictions are constrained to lie within this local view.

Alternatively, a set of methods [25], [26] utilizes previously observed trajectories of humans in the target scene to infer common motion patterns. While this can be helpful information to improve trajectory prediction, these approaches can not be easily transferred to zero-shot prediction in novel scenes.

Most related to us, Bruckschen *et al.* [27] use human-object interactions to predict human navigation goals and present a Bayesian inference framework to predict the goal of a human based on previously observed human-object interactions in the environment. However, this method only predicts goals instead of full trajectories and relies on previously observed interactions with the same objects.

Human Action Forecasting. The goal of human action forecasting is to predict human actions from visual input, often recorded in a egocentric perspective [28]. However, most methods specialize on highly specific domains (e.g., cooking) and datasets [29], [30]. As a consequence, many are restricted to a given vocabulary of actions and objects [31], [32] and can be hard to transfer to other domains or environments. Recently, Huang *et al.* [18] propose to use LLMs to anticipate human actions based on previous observations, outperforming other methods at the EGO4D LTA challenge 2023. This has the advantage that it can be applied to open-vocabulary scenarios and future actions can be inferred in a zero-shot manner.

Datasets for Human Trajectory Prediction. While there are many outstanding datasets for human trajectory prediction [2], [8]–[11], [33]–[41], the presented problem requires a number of specific attributes: trajectories need to extend over long time spans (≥ 60 s) and take place in complex and semantically rich human-centric environments, such as an office or a residential space. In addition, sensory data that allows the construction of a scene representation and rich annotations such as ground truth scenes, trajectories, and interactions should be provided.

Several datasets provide real-world human trajectories, but do not contain sensory data about the environment [8]–[11] and are often relatively short term. Other datasets cover longer time horizons and interactions with the environment, but are restricted to single-room, lab-like environments [33]–[36]. A third category of datasets [37]–[40] from the robotics domain observes parts of large environments, but does not record ground-truth human trajectories and focus mostly on social robot navigation, neglecting to record the parts of the environments where humans are likely to interact with objects and agents. To achieve detailed annotations, synthetic datasets have been recorded using game engines [2], [41], but mostly focus on joint-level trajectory prediction. In contrast, this work

¹Released at <https://github.com/MIT-SPARK/LP2> upon acceptance.

introduces a novel semi-synthetic dataset of 76 long-term trajectories (3 min) in two semantically rich environments.

III. PROBLEM STATEMENT

We address the task of long-term human trajectory prediction in semantically rich environments, given the human’s past trajectory, past interactions with the environment, and a model of that environment. We denote the future trajectory $\mathcal{T}_f = \{\mathbf{y}_{t+1}, \mathbf{y}_{t+2}, \dots, \mathbf{y}_{t+T}\}$ and past trajectory $\mathcal{T}_p = \{\mathbf{y}_{t-T_0}, \mathbf{y}_{t-T_0+1}, \dots, \mathbf{y}_t\}$, where $\mathbf{y}_i \in \mathbb{R}^2$ denotes the 2D position of the human at time i . We further assume that past human-object interactions A_p (encoded by the associated object), action description, and duration triples (e.g., {"sink", "wash hands", 12s}), and a scene representation S is given. Since many future trajectories are possible, the goal is to estimate a multi-modal spatio-temporal distribution $\mathbb{P}(\mathcal{T}_f|A_p, \mathcal{T}_p, S)$ over future trajectories \mathcal{T}_f given the past interactions A_p , past trajectory \mathcal{T}_p , and scene representation S . We assume there is a single human in the environment.²

IV. APPROACH

Our goal is to predict long-term future human trajectories, where humans may interact with several objects in the scene leading to sudden stopping or changes in moving direction. As there are many plausible objects to interact with and varying durations of these interactions, the prediction of a highly multi-modal distribution both in space and time is required.

To overcome these challenges, we propose a hierarchical approach that splits the task into high- and low-level reasoning parts. First, an *interaction sequence prediction* (ISP) module predicts sequences of likely future interactions A_f of the human in the environment. Second, a *probabilistic trajectory prediction* (PTP) module grounds these sequences into cohesive trajectories \mathcal{T}_f and predicts a continuous spatio-temporal probability distribution $\mathbb{P}(\mathcal{T}_f|A_f, A_p, \mathcal{T}_p, S)$ over the future human position. Formally, this reflects the assumption that humans are goal driven, *i.e.*, their trajectories are fully specified by their environment and goals, where goals in turn can be inferred from their previous activities:

$$\mathbb{P}(\mathcal{T}_f|A_p, \mathcal{T}_p, S) = \sum_{A_f} \underbrace{\mathbb{P}(\mathcal{T}_f|A_f, \mathcal{T}_p, S)}_{\text{PTP}} \underbrace{\mathbb{P}(A_f|A_p, \mathcal{T}_p, S)}_{\text{ISP}} \quad (1)$$

An overview of our approach is shown in Fig. 2. We detail each component below, after discussing our choice of scene representation.

Environment Representation. To effectively reason about complex scenes we choose 3D dynamic scene graphs (DSGs) [13], [14], [42] as a scene representation. A DSG provides a hierarchical symbolic abstraction, where each symbol is physically grounded in the scene. Formally, it consists of a set of nodes and edges $S = \{\mathcal{V}, \mathcal{E}\}$. The nodes $v \in \mathcal{V}$ are grouped into layers L , with inter- and intra-layer edges $e_{ij} \in \mathcal{E}$ specifying relationships between nodes v_i and v_j .

²While outside the scope of this work, we note that dynamic entities, such as other agents, could easily be included in the scene representation S .

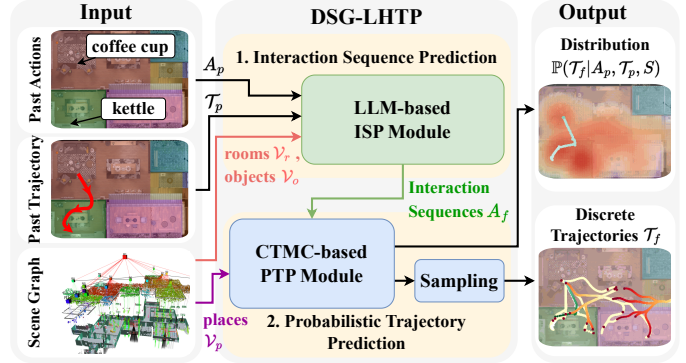


Fig. 2: Approach overview. The interaction sequence prediction (ISP) module estimates sequences of future interactions with the environment using the rich semantic information of the scene graph S . The probabilistic trajectory prediction (PTP) module connects these sequences into cohesive trajectories and predicts a continuous spatio-temporal probability distribution over the future human position in the environment.

We follow the definition of [15] with layers $L = \{o, p, r\}$ encoding objects o , places p , and rooms r , respectively. Notably, all nodes $v_o \in \mathcal{V}_o$ denote a semantic object in the scene, whereas all places $v_p \in \mathcal{V}_p$ and their intra-layer edges $e_{p_i p_j} \in \mathcal{E}$ represent the traversable free space in the scene.

While we assume the DSG S to be given in this work, it can also be constructed in real-time on a robot [15], [43].

Interaction Sequence Prediction. To estimate future interactions, we build on the grounded symbols in the DSG S and the zero-shot reasoning power of LLMs [17], [18]. Similar to Rana *et al.* [44], we first parse S into a natural language description of the scene \tilde{S} . In contrast to [44], we write full sentence descriptions of the environment, hierarchically describing all rooms $v_r \in \mathcal{V}_r$, connectivity between rooms $e_{r_i r_j} \in \mathcal{E}$, and objects $v_o \in \mathcal{V}_o \mid \exists e_{v_o v_r} \in \mathcal{E}$ in each room. We prompt the LLM to predict $W_I \in \mathbb{N}^+$ next interactions A_i and likelihoods $p_{act,i} \in (0, 1]$ of A_i occurring as well as estimated durations τ_i of A_i based on the description of the environment \tilde{S} and the past interactions A_p . We further prompt the LLM to provide reasoning about its prediction, which we empirically found to improve the prediction quality. The output is a JSON serializable dictionary of A_i , an example of which is shown as a green node in Fig. 3.

We consider two levels of granularity when predicting the objects of A_i , prompting the LLM to predict either only the *semantic class* s of the next object or the unique object *instance*. In the former case, we conjecture that humans are more likely to interact with close-by entities and consider the N_s closest instances of the predicted class s as target objects, where we additionally weight the predicted likelihood $p_{act,i}$ by the inverse distance. To simplify the LLM prediction task, we also condense the scene description \tilde{S} in this case for objects of each semantic class in a room into a single description, *e.g.*, “In the kitchen, there are 4 chairs”.

To predict a sequence of interactions, we build a tree T_I with the current position of the human as a root and all predicted

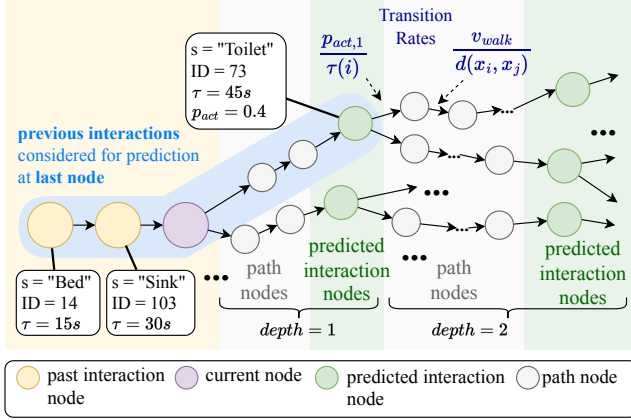


Fig. 3: Interaction sequence tree T_I . The LLM is auto-regressively prompted with the scene S and the previous interactions A_p to predict the next interactions (green nodes). Shortest paths spatially connect interactions (gray nodes). Progression through the tree over time is modeled as a CTMC with probability-based transition rates (blue). As time progresses, the probability mass moves from left to right.

next interactions as leaves. For each leaf in T_I , we auto-regressively prompt the LLM with the accumulated previous actions of the human to predict the following interactions, up to a *depth* of D_I . This results in up to $(W_I \times N_s)^{D_I}$ total considered interaction sequences.

Probabilistic Trajectory Prediction. Finally, we need to translate the interaction tree T_I into a spatio-temporal distribution of human positions. To ground the interaction predictions in spatial positions, we augment T_I with the traversability information captured in the places \mathcal{V}_p of S . Assuming humans are efficient in their paths, we find the shortest-path in \mathcal{E}_{pp} connecting each previous interaction to the possible following ones. A resulting tree is shown in Fig. 3, where each green node corresponds to a future interaction A_i , and gray nodes represent the traversable paths connecting them.

We model the human’s progression through this tree over time as a stochastic process and construct a continuous-time Markov chain (CTMC) [45]. The CTMC is defined by the state space X , given by the nodes of the interaction tree T_I , an initial state x_0 , and a transition matrix $Q \in \mathbb{R}^{|X| \times |X|}$. Initially, all probability mass is concentrated at the current position of the human $\mathbb{P}(x(0)) = \{1, 0^{|X|-1}\}$. We model the time it takes a human to traverse a path as an exponential distribution where the mean is the distance divided by the average human walking speed v_{walk} . Similarly, we model the duration of an interaction A_i as an exponential distribution based on the predicted duration τ_i . The transition matrix can thus be constructed as:

$$Q_{i,j} = \begin{cases} \frac{v_{walk}}{d(x_i, x_j)} & \text{if } x_i \text{ \& } x_j \text{ are path nodes} \\ \frac{p_{act,j}}{\tau_i} & \text{if } i \text{ is an interaction node} \\ \sum_{x_i \in X, i \neq j} -Q_{i,j} & \text{if } i = j \\ 0 & \text{else} \end{cases}, \quad (2)$$

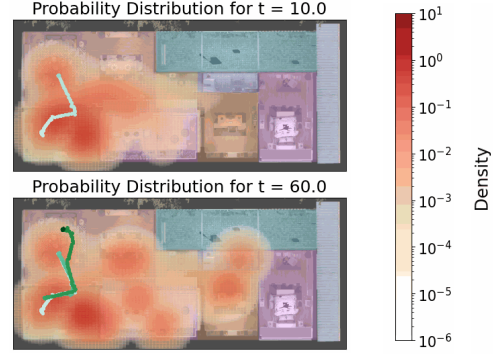


Fig. 4: Spatio-temporal distribution over the human’s predicted position (orange) progressing through time. True trajectory colored from light at $t = 0s$ to dark at $t = 60s$ green.

where $d(x_i, x_j)$ is the Euclidean distance between nodes x_i and x_j . To infer the probability distribution $\mathbb{P}(x(t))$ of the human being at state x at time t , we solve the Kolmogorov forward equation [45] given by

$$\frac{\partial}{\partial t} \mathbb{P}(x(t)) = Q \cdot \mathbb{P}(x(t)). \quad (3)$$

The solution to this equation is

$$\mathbb{P}(x(t)) = \exp(Q(t - t_0)) \mathbb{P}(x_0). \quad (4)$$

As our structure of the CTMC is a tree, the transition matrix Q is triangular and the exponential can be computed efficiently.

To also consider spatial uncertainty, we model the probability of the human being in physical space ξ at time t as a mixture of Gaussians with positions x , weights $\mathbb{P}(x(t))$, and an empirically determined kernel width. An example of the resulting spatio-temporal distribution is shown in Fig. 4.

Implementation Details. We use GPT-4-turbo [46] as a state-of-the-art LLM in our ISP module. The configurable ISP hyperparameters are set to $W_I = 6$, $D_I = 2$, and $N_s = 3$, resulting in up to 324 considered future interaction sequences.

V. DATASET

As there currently exist no datasets for our task, a novel semi-synthetic dataset is created. We consider two typical environments: a large office and a smaller home scene. They span 13 rooms with 107 objects over 994m² and 9 rooms with 120 objects over 111m², respectively. To create realistic and diverse trajectories, we generate interaction sequences by human annotators, crowd-sourced through Amazon Mechanical Turk. To achieve coherent and realistic trajectories, annotators are prompted to envision sequences of interactions with objects in a pictured scene while fulfilling an abstract task in that scene. Interactions are annotated with estimates of interaction times, action descriptions, and a description of the human’s higher-level goal. We manually verify the quality of all submissions. We then simulate SMPL human shape models [47] fulfilling these sequences of interactions in TESSE [48], a high-fidelity simulator based on unity.

Our dataset covers a wide range of scenarios, including trajectories that start while the human is interacting as well

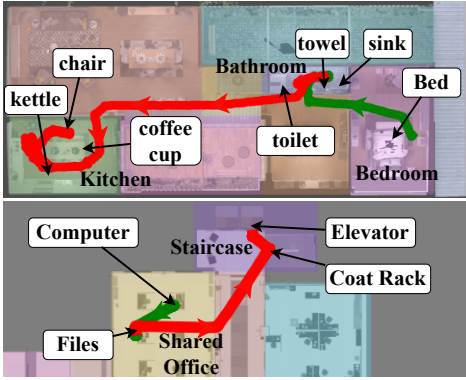


Fig. 5: Example trajectories in the home (top) and office (bottom). Trajectory is shown in green (past) and red (future).

Attribute	Office	Home
#Trajectories that start while interacting [1]	11	14
#Trajectories that start while walking [1]	34	17
Distance travelled in past [m]	14.0±11.9	7.8±3.0
Distance travelled in future [m]	18.6±12.7	11.7±6.5
#Past interactions [1]	2.2±0.5	2.4±0.5
#Future interactions [1]	2.3±0.8	2.2±0.8
Duration of past observation [s]	67.6± 30.8	60.6±30.2
Time spent interacting in past [s]	55.2±30.1	55.1±30.4
Time spent interacting in future [s]	43.7±11.5	51.3±6.6

Table I: Diverse characteristics of our newly recorded dataset.

as when the human is moving in between interactions. To prevent bias towards the start point, we split trajectories into past/future after the second interaction or 60s before the end of the full recorded trajectory, whichever comes first. This way, we focus on the part of the trajectory that is relevant to most applications. The dataset contains a total of 76 trajectories, whose diverse characteristics are shown in Tab. I. Example trajectories are shown in Fig. 5.

VI. EXPERIMENTS

We aim to answer the following questions:

- 1) How does the performance of LP^2 compare to prior art in long-term human trajectory prediction?
- 2) How long does the trajectory prediction stay meaningful?
- 3) How does interaction duration impact task difficulty?
- 4) How accurate is the LLM ISP, and how does predicting instances compare to our method using semantic classes?
- 5) What is the benefit of our CTMC-based PTP module in comparison to directly predicting full-length trajectories?

Experimental Setup. In order to focus on the performance of the trajectory prediction, a DSG S is constructed for each scene based on ground-truth semantic information provided by the simulator. Akin to relational action forecasting [31], we separate the task of predicting future actions from action recognition and assume the past interactions to be given. We note that when engineering an end-to-end system, a DSG and past interactions could be estimated using approaches like [15], [49], [50], but engineering such a system is currently out of scope for this work. Due to the different scales of the environments we evaluate each one separately.

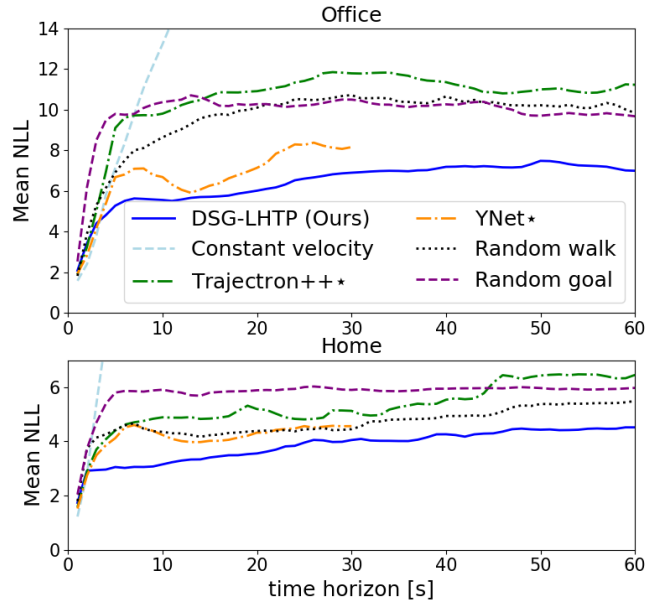


Fig. 6: Negative log-likelihood evolving over time.

Metrics. We evaluate the ability to predict multi-modal spatio-temporal distributions by computing the *negative log likelihood* (NLL) of the ground truth future trajectory in the predicted distribution. We further compute the *best-of-N average displacement error* (BoN ADE), reporting the lowest mean squared error between of N discrete predicted trajectories and the ground truth. Both metrics are computed over a time horizon of 60s and lower is better.

Baselines. Comparing our method to prior art in long-term human trajectory prediction is challenging, as most methods rely on training their models on extensive datasets. As we are not aware of other datasets that provide human trajectories over 60s, we train these methods on existing datasets with a shorter time horizon and fine tune them on our dataset. We compare against *Trajectron++* [7] and *YNet* [12], two state-of-the-art methods for human trajectory forecasting. We train *Trajectron++* on the ETH and UCY datasets [8], [9], including occupancy maps of the dataset scenes as scene input. Additionally, we fine tune the model on the hold-out scenes of our dataset. Since *YNet*'s architecture requires a fixed prediction horizon, we train it on the Stanford drones dataset [11] providing trajectories up to 30s into the future. We also include occupancy maps of the dataset scenes as input and fine tune *YNet* on our dataset for fair comparison. Note that our method has not seen any data of our dataset while both of the baselines can be considered privileged. We further compare to a constant velocity model based on the current direction and velocity of the human, and also provide a *random walk* and motion towards a *random goal* within the places of the scene graph as references. The NLL of these baselines is measured as for our method by performing Kernel Density Estimation (KDE) over the predicted trajectories for each timestep.

1) Long-term Trajectory Prediction Performance. To investigate the ability to predict multi-modal spatio-temporal

distributions over complex human trajectories, we show the average NLL vs. future time in each environment in Fig. 6. We observe that for short horizons of ~ 4 s most methods achieve similar performance. The only outlier is *random goal*, which in some cases may send the prediction off into a wrong direction. However, as the prediction horizon increases our approach shows superior performance compared to all baselines. Notably, the NLL only increases gradually for LP^2 , demonstrating its ability to support multi-modal long-horizon distributions. In contrast, most other methods quickly saturate at an uninformative state as indicated by the *random goal* baseline. This can be explained by the fact that in our setting, where trajectories are less unidirectional and homogeneous, Trajectron++ and YNet struggle to account for sudden stops or changes in walking direction. While it may seem counter-intuitive that the *random walk* performs strongly, this represents an inherent bias in humans often times not moving very far away from their starting point when accomplishing a task. As expected, this is more pronounced for the smaller home environment.

We further show the Bo5 and Bo20 ADE at 60s into the future for methods that output discrete trajectories in Tab. II. We observe that LP^2 shows strong performance for ADE over the entire length of 60s, most pronounced for the multi-modal Bo20 setting. The baseline methods show better performance early, which is the domain they specialize in. While our method does not focus on taking the past trajectory much into account for accurate prediction of the immediate next trajectory, we believe that such approaches can be combined with our long-term predictions. It is also worth pointing out that due to our tree-structured ISP, multiple of the most likely trajectories may have the same first interaction, reducing the breadth of our early prediction. Finally, both Ynet and Trajectron++ can achieve strong performance when fine tuned on the hold-out scenes of the dataset. However, the performance is notably decreased without this additional domain knowledge, whereas LP^2 achieves accurate predictions in a zero-shot manner.

2) Time Horizon of Meaningful Prediction. A central challenge in long-term human trajectory prediction is the fast growth of possible positions with time. First, the NLL in Fig. 6 indicates that our prediction remains relevant for the entire 60s. Nonetheless, we further analyze this limit by inspecting the progression of probability mass through the CTMC by comparing the distribution $\mathbb{P}(x(t))$ to the steady state distribution $\mathbb{P}(x_{steady})$ that satisfies $Q \cdot \mathbb{P}(x_{steady}) = 0$. We find that after 69.9s in the home and 93.0s in the office environment, the total variation distance $D_{TV}(\mathbb{P}(x(t)), \mathbb{P}(x_{steady}))$ is below 0.5, *i.e.*, the majority of the predicted probability $\mathbb{P}(x(t))$ is static in the leaf nodes of the interaction sequence tree. Interestingly, we experimentally find that the NLL for this quasi-static prediction is still lower than that of the *random goal*. This indicates that the steady state prediction of our model acts like a static prior about which objects humans are most likely to interact with in general. However, although such a prior can be useful in many cases, it no longer reflects

Scene	Metric	Bo5 ADE [m]			Bo20 ADE [m]		
		Timeframe [s]	0-10	10-30	30-60	0-10	10-30
Office	Trajectron++*	2.60	5.30	6.94	2.55	4.93	6.25
	YNet*	2.34	4.64	-	1.92	2.35	-
	Trajectron++	2.75	8.34	16.4	<u>2.42</u>	5.90	10.9
	YNet	3.41	9.63	-	3.05	8.07	-
	Const. Vel.	<u>2.67</u>	10.6	23.7	2.67	10.6	23.7
	LP^2 (Ours)	3.04	<u>6.38</u>	<u>7.70</u>	3.00	<u>4.43</u>	4.06
Home	Trajectron++*	1.39	1.59	1.99	1.33	1.34	1.67
	YNet*	1.40	2.04	-	1.33	1.30	-
	Trajectron++	2.23	6.51	14.3	1.67	4.03	8.94
	YNet	1.46	1.95	-	1.34	1.43	-
	Const. Vel.	2.80	11.0	25.5	2.80	11.0	25.5
	LP^2 (Ours)	1.22	1.42	1.56	1.06	1.20	1.37

Table II: BoN ADE for different time horizons. *Denotes privileged methods fine-tuned on hold-out scenes. Best number shown in bold, best non-privileged number in underline.

a trajectory prediction. We note that a dynamic prediction beyond this horizon is in principle possible by increasing the depth of the ISP module, however, how long the main modes of the prediction stay meaningful depends on the complexity of the environment and task the human is planing to achieve.

3) Importance of the Interaction Duration. A key challenge of the task is that a human may interact with entities in the environment for an extended duration, disrupting traditional trajectory prediction methods. For example, a human might interact with a sink for 15s when washing their hands, but 3 min when washing dishes (the action label in both cases may just be “washing”). Having to predict the interaction duration τ_i adds additional complexity and variance to the LHTP task. To investigate the impact of this, we study the performance of our method when disregarding the interaction times and predicting only the movement in between interactions. We find that having to account for the interaction duration increases the NLL on average by 25.5% in the home and 31.7% in the office scene. Although our ISP module accounts for some of the uncertainty in duration prediction by modeling it as an exponential distribution rather than a single estimated value, this highlights the highly complex nature of our problem on top of estimating the correct interactions.

4) Object Instance vs. Semantic Class Prediction. To analyze our strategy of simplifying the prediction task for the LLM by predicting only the semantic class of next interactions and reasoning about the specific instance spatially (Sec. IV), we compare it to directly predicting the object instance. Tab. III shows performance metrics if the *semantic* class or *instance* id is predicted (pred.) or known (GT). Naturally, knowing the true instance the human will interact with achieves the best performance. This is most pronounced for $t = 30 - 60$ s, as predicting interactions far ahead is challenging. Nonetheless, knowing the true semantic class already provides a lot of information and results in only moderately worse performance.

Metric	Avg. NLL [-]			Bo5 ADE [m]			Bo20 ADE [m]		
	<10	<30	<60	<10	<30	<60	<10s	<30	<60
Semantic-Pred.	<u>3.60</u>	<u>4.86</u>	<u>5.72</u>	<u>2.51</u>	<u>4.87</u>	<u>5.25</u>	<u>2.28</u>	<u>3.71</u>	<u>3.54</u>
Instance-Pred.	4.23	6.52	7.63	2.67	6.48	9.00	2.67	6.25	7.35
Semantic-GT	3.11	3.60	4.21	2.65	4.51	4.44	2.37	3.45	3.15
Instance-GT	2.92	3.14	3.33	2.09	2.98	1.97	2.09	2.98	1.97

Table III: Performance metrics for class vs. instance prediction. Best number shown bold, best non-GT number underlined.

Scene	Metric	Top-10 Instance Acc. [%]		Top-10 Semantic Acc. [%]	
		First	Second	First	Second
Office	Semantic-Pred.	55.6	38.7	71.1	81.3
	Instance-Pred.	35.5	29.0	71.1	83.9
Home	Semantic-Pred.	56.7	40.0	60.0	46.7
	Instance-Pred.	43.3	53.3	50.0	53.3

Table IV: Top-10 accuracy of the predicted object interactions.

In contrast, when these qualities have to be predicted, we see the inverse trend. As the LLM performs notably better at predicting only the semantic class compared to the specific instance, the optimality gap is much smaller in the semantic case, indicating better trajectory prediction. To isolate the ISP prediction performance, we also report the top-10 accuracy, *i.e.*, how often the true interaction is among the 10 most likely predictions, in Tab. IV. We observe that predicting the right instance out of 120 and 107 objects in the home and office, respectively, is challenging. In the office, the difference is more pronounced as there are more objects of the same class.

5) Deterministic Prediction vs. Probabilistic CTMC. To evaluate how the CTMC improves our modeling of the progression of the probability distribution through time, we compare our method to a similar, but deterministic baseline that uses the identical interaction predictions as our method in Tab. V. Rather than modeling the trajectory evolution probabilistically using a CTMC, it directly infers full trajectories from the auto-regressive prediction and deterministically “walks” along these trajectory as time progresses. This shows that by using the CTMC framework and thereby modeling uncertainties like the human’s walking speed and interaction times with the objects in the environment as exponentially distributed probabilistic variables, we can improve our prediction.

VII. LIMITATIONS

While our method shows promising performance for long-horizon predictions, it does not yet make optimal use of all available information to refine the early part of the trajectory. While integrating learning-based methods like [7], [12] might work well, considering additional input modalities like eye

Metric	Avg. NLL [-]			Bo5 ADE [m]			Bo20 ADE [m]		
	<10	<30	<60	<10	<30	<60	<10s	<30	<60
CTMC	3.60	4.86	5.72	2.51	4.87	5.25	2.28	3.71	3.54
Deterministic	4.41	6.25	6.66	2.61	4.98	5.30	2.30	3.74	3.60

Table V: Performance metrics for deterministic vs. CTMC-based trajectory prediction.

gaze and audio-visual signals could be highly beneficial to improve motion and interaction prediction. Further, we currently only consider interactions at a single location. Extending this to interactions that cover a larger area (e.g., sweeping the floor in a room) would be of interest. Another limitation is that the current approach may not scale well to very high interaction prediction depths, as the tree size grows exponentially and Q is quadratic in the tree size. This could be addressed by more selectively rolling out high-probability interactions. Finally, we currently only consider a single agent. Expanding our approach to multi-agent scenarios presents an exciting opportunity to explore the complex dynamics of multiple interacting agents and the impact of social influences on long-term trajectories. We believe the methodology of using *dynamic* scene graphs can extend to moving entities and interactions with them.

VIII. CONCLUSION

In this work, we explored the problem of long-term human trajectory prediction of up to 60s, including human-object interactions. We presented LP^2 , a novel approach composed of a LLM-based module to predict human-object interactions and a CTMC-based probabilistic planning method that grounds these interaction sequences into a spatio-temporal distribution over future human positions. We introduced a novel semi-synthetic dataset of human trajectories in indoor environments annotated with rich human-object interactions and long-horizon trajectories. We show in a thorough experimental evaluation that our method outperforms prior art in long-term human trajectory prediction methods, especially as the time horizon extends beyond 20s and when dealing with trajectories that include complex interactions with the environment. We show, that we can predict a meaningful distribution of the human’s future location for a horizon up to 60s and highlight the importance of modeling the temporal nature of the interactions with the environment. We will release our code and dataset to facilitate further research in this area.

REFERENCES

- [1] A. Rudenko, L. Palmieri, M. Herman, K. M. Kitani, D. M. Gavrila, and K. O. Arras, “Human motion trajectory prediction: A survey,” *Intl. J. of Robotics Research*, vol. 39, no. 8, pp. 895–935, 2020.
- [2] Z. Cao, H. Gao, K. Mangalam, Q.-Z. Cai, M. Vo, and J. Malik, “Long-term human motion prediction with scene context,” in *European Conf. on Computer Vision (ECCV)*. Springer, 2020, pp. 387–404.
- [3] K. Mangalam, H. Girase, S. Agarwal, K.-H. Lee, E. Adeli, J. Malik, and A. Gaidon, “It is not the journey but the destination: Endpoint conditioned trajectory prediction,” in *European Conf. on Computer Vision (ECCV)*, 2020, pp. 759–776.
- [4] T. Salzmann, L. Chiang, M. Ryll, D. Sadigh, C. Parada, and A. Bewley, “Robots that can see: Leveraging human pose for trajectory prediction,” *IEEE Robotics and Automation Letters*, vol. 8, no. 11, pp. 7090–7097, 2023.
- [5] A. Sadeghian, V. Kosaraju, A. Sadeghian, N. Hirose, H. Rezatofighi, and S. Savarese, “Sophie: An attentive gan for predicting paths compliant to social and physical constraints,” in *IEEE Conf. on Computer Vision and Pattern Recognition (CVPR)*, 2019, pp. 1349–1358.
- [6] Y. Yuan, X. Weng, Y. Ou, and K. M. Kitani, “Agentformer: Agent-aware transformers for socio-temporal multi-agent forecasting,” in *Intl. Conf. on Computer Vision (ICCV)*, 2021, pp. 9813–9823.
- [7] T. Salzmann, B. Ivanovic, P. Chakravarty, and M. Pavone, “Trajectron++: Dynamically-feasible trajectory forecasting with heterogeneous data,” in *European Conf. on Computer Vision (ECCV)*, 2020, pp. 683–700.

- [8] S. Pellegrini, A. Ess, K. Schindler, and L. Van Gool, "You'll never walk alone: Modeling social behavior for multi-target tracking," in *Intl. Conf. on Computer Vision (ICCV)*. IEEE, 2009, pp. 261–268.
- [9] A. Lerner, Y. Chrysanthou, and D. Lischinski, "Crowds by example," in *Computer graphics forum*, vol. 26, no. 3. Wiley Online Library, 2007, pp. 655–664.
- [10] D. Bršćić, T. Kanda, T. Ikeda, and T. Miyashita, "Person tracking in large public spaces using 3-d range sensors," *IEEE Trans. on Human-Machine Systems*, vol. 43, no. 6, pp. 522–534, 2013.
- [11] A. Robicquet, A. Sadeghian, A. Alahi, and S. Savarese, "Learning social etiquette: Human trajectory understanding in crowded scenes," in *European Conf. on Computer Vision (ECCV)*, 2016, pp. 549–565.
- [12] K. Mangalam, Y. An, H. Girase, and J. Malik, "From goals, waypoints & paths to long term human trajectory forecasting," in *Intl. Conf. on Computer Vision (ICCV)*, 2021, pp. 15 233–15 242.
- [13] I. Armeni, Z. He, J. Gwak, A. Zamir, M. Fischer, J. Malik, and S. Savarese, "3D scene graph: A structure for unified semantics, 3D space, and camera," in *Intl. Conf. on Computer Vision (ICCV)*, 2019, pp. 5664–5673.
- [14] A. Rosinol, A. Violette, M. Abate, N. Hughes, Y. Chang, J. Shi, A. Gupta, and L. Carlone, "Kimeria: from SLAM to spatial perception with 3D dynamic scene graphs," *Intl. J. of Robotics Research*, vol. 40, no. 12–14, pp. 1510–1546, 2021.
- [15] N. Hughes, Y. Chang, S. Hu, R. Talak, R. Abdulhai, J. Strader, and L. Carlone, "Foundations of spatial perception for robotics: Hierarchical representations and real-time systems," *Intl. J. of Robotics Research*, 2024.
- [16] S. Looper, J. Rodriguez-Puigvert, R. Siegwart, C. Cadena, and L. Schmid, "3d vsg: Long-term semantic scene change prediction through 3d variable scene graphs," in *IEEE Intl. Conf. on Robotics and Automation (ICRA)*. IEEE, 2023, pp. 8179–8186.
- [17] J. S. Park, J. C. O'Brien, C. J. Cai, M. R. Morris, P. Liang, and M. S. Bernstein, "Generative agents: Interactive simulacra of human behavior," in *ACM Symp. on User Interface Software and Technology (UIST)*, 2023.
- [18] D. Huang, O. Hilliges, L. Van Gool, and X. Wang, "Palm: Predicting actions through language models @ ego4d long-term action anticipation challenge," *arXiv preprint arXiv:2306.16545*, 2023.
- [19] S. Kim, D. Huang, Y. Xian, O. Hilliges, L. Van Gool, and X. Wang, "Lalm: Long-term action anticipation with language models," *arXiv preprint arXiv:2311.17944*, 2023.
- [20] N. Lee, W. Choi, P. Vernaza, C. B. Choy, P. H. Torr, and M. Chandraker, "Desire: Distant future prediction in dynamic scenes with interacting agents," in *IEEE Conf. on Computer Vision and Pattern Recognition (CVPR)*, 2017, pp. 336–345.
- [21] T. Fernando, S. Denman, S. Sridharan, and C. Fookes, "Neighbourhood context embeddings in deep inverse reinforcement learning for predicting pedestrian motion over long time horizons," in *Intl. Conf. on Computer Vision (ICCV) Workshops*, 2019.
- [22] H. Tran, V. Le, and T. Tran, "Goal-driven long-term trajectory prediction," in *IEEE Workshop on Applications of Computer Vision (WACV)*, 2021, pp. 796–805.
- [23] A. Gupta, J. Johnson, L. Fei-Fei, S. Savarese, and A. Alahi, "Social gan: Socially acceptable trajectories with generative adversarial networks," in *IEEE Conf. on Computer Vision and Pattern Recognition (CVPR)*, 2018, pp. 2255–2264.
- [24] A. Mohamed, K. Qian, M. Elhoseiny, and C. Claudel, "Social-stgcn: A social spatio-temporal graph convolutional neural network for human trajectory prediction," in *IEEE Conf. on Computer Vision and Pattern Recognition (CVPR)*, 2020, pp. 14 424–14 432.
- [25] Y. Zhu, A. Rudenko, T. P. Kucner, L. Palmieri, K. O. Arras, A. J. Lilienthal, and M. Magnusson, "Cliff-lhmp: Using spatial dynamics patterns for long-term human motion prediction," in *IEEE/RSJ Intl. Conf. on Intelligent Robots and Systems (IROS)*. IEEE, 2023, pp. 3795–3802.
- [26] Y. Zhu, H. Fan, A. Rudenko, M. Magnusson, E. Schaffernicht, and A. J. Lilienthal, "Lace-lhmp: Airflow modelling-inspired long-term human motion prediction by enhancing laminar characteristics in human flow," *arXiv preprint arXiv:2403.13640*, 2024.
- [27] L. Bruckschen, K. Bungert, N. Dengler, and M. Bennewitz, "Predicting human navigation goals based on bayesian inference and activity regions," *Robotics and Autonomous Systems*, vol. 134, p. 103664, 2020.
- [28] Y. Kong and Y. Fu, "Human action recognition and prediction: A survey," *Intl. J. of Computer Vision*, vol. 130, no. 5, pp. 1366–1401, 2022.
- [29] D. Damen, H. Doughty, G. M. Farinella, S. Fidler, A. Furnari, E. Kazakos, D. Moltisanti, J. Munro, T. Perrett, W. Price *et al.*, "Scaling egocentric vision: The epic-kitchens dataset," in *European Conf. on Computer Vision (ECCV)*, 2018, pp. 720–736.
- [30] F. Sener, D. Chatterjee, D. Shelepov, K. He, D. Singhania, R. Wang, and A. Yao, "Assembly101: A large-scale multi-view video dataset for understanding procedural activities," in *IEEE Conf. on Computer Vision and Pattern Recognition (CVPR)*, 2022, pp. 21 096–21 106.
- [31] C. Sun, A. Shrivastava, C. Vondrick, R. Sukthankar, K. Murphy, and C. Schmid, "Relational action forecasting," in *IEEE Conf. on Computer Vision and Pattern Recognition (CVPR)*, June 2019.
- [32] Y. Abu Farha, A. Richard, and J. Gall, "When will you do what? - anticipating temporal occurrences of activities," in *IEEE Conf. on Computer Vision and Pattern Recognition (CVPR)*, June 2018.
- [33] A. Rudenko, T. P. Kucner, C. S. Swaminathan, R. T. Chadalavada, K. O. Arras, and A. J. Lilienthal, "Thör: Human-robot navigation data collection and accurate motion trajectories dataset," *IEEE Robotics and Automation Letters*, vol. 5, no. 2, pp. 676–682, 2020.
- [34] T. R. de Almeida, A. Rudenko, T. Schreiter, Y. Zhu, E. G. Maestro, L. Morillo-Mendez, T. P. Kucner, O. M. Mozos, M. Magnusson, L. Palmieri *et al.*, "Thor-magni: Comparative analysis of deep learning models for role-conditioned human motion prediction," in *Intl. Conf. on Computer Vision (ICCV)*, 2023, pp. 2200–2209.
- [35] M. N. Finean, L. Petrović, W. Merkt, I. Marković, and I. Havoutis, "Motion planning in dynamic environments using context-aware human trajectory prediction," *Robotics and Autonomous Systems*, vol. 166, p. 104450, 2023.
- [36] M. Hassan, V. Choutas, D. Tzionas, and M. J. Black, "Resolving 3D human pose ambiguities with 3D scene constraints," in *Intl. Conf. on Computer Vision (ICCV)*, 2019, pp. 2282–2292.
- [37] Z. Yan, T. Duckett, and N. Bellotto, "Online learning for human classification in 3d lidar-based tracking," in *IEEE/RSJ Intl. Conf. on Intelligent Robots and Systems (IROS)*, 2017.
- [38] R. Martin-Martin, M. Patel, H. Rezatofighi, A. Sheno, J. Gwak, E. Frankel, A. Sadeghian, and S. Savarese, "Jrdb: A dataset and benchmark of egocentric robot visual perception of humans in built environments," *IEEE Trans. Pattern Anal. Machine Intell.*, 2021.
- [39] H. Karnan, A. Nair, X. Xiao, G. Warnell, S. Pirk, A. Toshev, J. Hart, J. Biswas, and P. Stone, "Socially compliant navigation dataset (scand): A large-scale dataset of demonstrations for social navigation," *IEEE Robotics and Automation Letters*, 2022.
- [40] Y. F. Chen, M. Everett, M. Liu, and J. P. How, "Socially aware motion planning with deep reinforcement learning," in *IEEE/RSJ Intl. Conf. on Intelligent Robots and Systems (IROS)*, 2017, pp. 1343–1350.
- [41] M. Hassan, D. Ceylan, R. Villegas, J. Saito, J. Yang, Y. Zhou, and M. Black, "Stochastic scene-aware motion prediction," in *Intl. Conf. on Computer Vision (ICCV)*, Oct. 2021.
- [42] A. Rosinol, A. Gupta, M. Abate, J. Shi, and L. Carlone, "3D dynamic scene graphs: Actionable spatial perception with places, objects, and humans," in *Robotics: Science and Systems (RSS)*, 2020.
- [43] N. Hughes, Y. Chang, and L. Carlone, "Hydra: a real-time spatial perception engine for 3D scene graph construction and optimization," in *Robotics: Science and Systems (RSS)*, 2022.
- [44] K. Rana, J. Haviland, S. Garg, J. Abou-Chakra, I. Reid, and N. Suenderhauf, "Sayplan: Grounding large language models using 3d scene graphs for scalable task planning," in *Conference on Robot Learning (CoRL)*, 2023.
- [45] J. R. Norris, *Markov chains*. Cambridge university press, 1998, no. 2.
- [46] OpenAI, "Gpt-4 technical report," *arXiv preprint arXiv:2303.08774*, 2023.
- [47] M. Loper, N. Mahmood, J. Romero, G. Pons-Moll, and M. J. Black, "SMPL: A skinned multi-person linear model," *ACM Trans. Graphics (Proc. SIGGRAPH Asia)*, vol. 34, no. 6, pp. 248:1–248:16, Oct. 2015.
- [48] Z. Ravichandran, J. D. Griffith, B. Smith, and C. Frost, "Bridging scene understanding and task execution with flexible simulation environments," *arXiv preprint arXiv:2011.10452*, 2020.
- [49] L. M. Dang, K. Min, H. Wang, M. J. Piran, C. H. Lee, and H. Moon, "Sensor-based and vision-based human activity recognition: A comprehensive survey," *Pattern Recognition*, vol. 108, p. 107561, 2020.
- [50] C. Feichtenhofer, Y. Li, K. He *et al.*, "Masked autoencoders as spatiotemporal learners," *Advances in Neural Information Processing Systems (NIPS)*, vol. 35, pp. 35 946–35 958, 2022.